Journal of Engineering Science and Technology
9th EURECA 2017 Special Issue September (2018) 52 - 62

SGO AND TSALLIS ENTROPY ASSISTED SEGMENTATION OF ABNORMAL REGIONS FROM BRAIN MRI

K. SURESH MANIC*, NAWF AL SHIBLI, RAHMA AL SULAIMI

Department of Electrical & Computer Engineering, Caledonian College of Engineering, University College, Muscat, Sultanate of Oman,
*Corresponding Author: suresh.manic@caledonian.edu.om

Abstract

Brain abnormality is an aggressive disease in humans. Premature detection may diminish the harshness of disease and also reduce the death rate. In this paper, heuristic algorithm supported computerized practice is proposed to segment/evaluate the abnormal section of brain Magnetic Resonance Images (MRI). Integration of the Social-Group-Optimization (SGO) and Tsallis-Entropy is implemented to enhance the feature of tumor section and the Localized Active Contour (LAC) is used to extract the tumor. Experiments are executed with Matlab software and benchmark brain MRI called BRATS 2015 database is adopted. The superiority of proposed technique is confirmed against the ground truth images. The competence of implemented technique is established with picture likeliness values, such as Jaccard and Dice; also statistical trials, like precession, sensitivity, specificity and accuracy. The outcome of the LAC is also compared against segmentation schemes, like the Watershed (WS) and Level Set (LS) procedures. The results of SGO+LAC outperform SGO+WS and SGO+LS approaches. The results confirm that, SGO+LAC supports better tumor extraction from MRI images recorded with Flair modality.

Keywords: Active contour, Brain tumor; MRI; Social group optimization algorithm.

1. Introduction

Computer assisted illness evaluation is generally considered in medicinal domain to determine illness with medical pictures. Therapeutic imaging actions will maintain the premature recognition with examination of a collection of infections and moreover helps to lessen the death rates.

In literature, substantial measures are discussed and applied to mine important details in conventional and medicinal pictures [1-6].

Heuristic approach aided picture processing is extensively considered in current days because of its effortlessness and lenience in execution [7, 8]. Tsallis-Entropy (TE) is one of the procedures, largely adopted by most of the researchers because of its dominance and elasticity [9, 10]. Previous works substantiate that, TE supported thresholding was mostly adopted by the researchers to extract important features from RGB/gray test pictures [5, 11-13].

Despotović et al. [14] recommends the segmentation challenges and the available procedures in the brain image processing approaches. This work also notifies that, grouping of numerous procedures is necessary to attain improved result [9].

In the literature, a number of automated and semi-automated approaches are existing to examine brain MRI recorded with a chosen modality. All the existing methods are modality specific approaches and the method works well with a chosen modality sometimes may fail to offer better outcome with other modalities. Moreover, the soft-computing assisted approaches will enhance the outcome of the disease examination procedure. Therefore, here a method using SGO aided thresholding is implemented to examine the brain MRI registered with the Flair modality.

In this paper, tri-level thresholding using SGO+TE is implemented to improve cancerous division of brain image. TE was originally projected in 1988 [9]. Grouping of TE and heuristic schemes has been existing for image thresholding [15]. Later, the Localized Active Contour (LAC) [16] segmentation is implemented to extort suspicious/enhanced region of brain MRI.

The capability of proposed segmentation task is then confirmed by means of a relative assessment between the segmented tumor area and expert's Ground Truth (GT). The experimental results verify that, implemented technique is capable in attaining improved picture likeness index [17] and statistical trials [18].

The outcome of implemented method is also authenticated with the other segmentation approaches, such as WS and LS. This investigational work confirms that, the overall outcome of the proposed SGO+LAC is better compared with the SGO+WS and SGO+LS.

2. Methodology

This division explains various stages involved in soft-computing assisted disease examination tool proposed in this work.

2.1. Pre-processing

Initially, a pre-processing technique is executed by combining of the Social Group Optimization (SGO) and the TE value. Usually, entropy is linked with the estimation of confusion inside an image. Shannon's theory guaranteed that, when a bodily structure is separated as two statistically open sub-systems like '*U'* and '*V'*, then the entropy value will be [9, 10]:

$$S(U+V) = S(U) + S(V) \tag{1}$$

Then, TE will be:

$$S_q = \frac{1-\sum_{i=1}^{T}(p_i)^q}{q-1} \tag{2}$$

where T = structure's possibility and q=entropic directory.

Eq. (2) forms Shannon-entropy when $q \to 1$.

The final entropy is:

$$S_q(U+V) = S_q(U) + S_q(V) + (1-q).S_q(U).S_q(V) \tag{3}$$

TE provides optimal threshold for image.

Let, image has L-gray values of range {0, 1, ..., L-1}, through likelihood allocation $p_i = p_0, p_1, ..., p_{L-1}$.

TE is expressed as:

$$f(T)=[T_1,T_2, \ldots , T_k] = argmax \left[S_q^U(T)+S_q^V(T)+\ldots+S_q^K(T)+(1-q).S_q^U(T).S_q^V(T)\ldots S_q^K(T)\right] \tag{4}$$

where

$$S_q^U(T) = \frac{1-\sum_{i=0}^{t_1-1}\left(\frac{Pi}{P^U}\right)^q}{q-1}, \; P^U = \sum_{i=0}^{t_1-1} Pi$$

$$S_q^V(T) = \frac{1-\sum_{i=t_1}^{t_2-1}\left(\frac{Pi}{P^V}\right)^q}{q-1}, \; P^V = \sum_{i=t_1}^{t_2-1} Pi$$

$$S_q^K(T) = \frac{1-\sum_{i=t_k}^{L-1}\left(\frac{Pi}{P^K}\right)^q}{q-1}, \; P^K = \sum_{i=t_k}^{L2-1} Pi$$

In this practice, optimal threshold value T is obtained by maximizing $f(T)$. Implemented effort finds the arbitrary values of the T based on the heuristic search by the SGO algorithm. The threshold level is assigned as T =3 [19-22], with probabilities P^A, P^B, and P^C. The heuristic search continuously explores the gray level thresholds of the chosen MRI threshold and computes the value of $f(T)$. This process continues until the search converges with a maximized value of the $f(T)$ or until the maximum iteration value is reached. At the end of the search, the SGO obtains the required value of the thresholds and the maximized entropy function $f(T)$.

SGO is developed by Satapathy and Naik [23] in 2016. SGO has two-phases:

i. Recovering period

Let X is the group of members, like i = 1, 2,…, N and D = search dimension with j = 1, 2, …, D.

$$Xnew_{i,j} = CXold_{i,j} + r(gbest_j - Xold_{i,j}) \tag{5}$$

ii. Gaining period

$$Xnew_{i,j} = Xold_{i,j} + r_1 * (X_{i,j} - X_{r,j}) + r_2 * (gbest_j - X_{i,j}) \quad (6)$$

$$Xnew_{i,:} = Xold_{i,:} + r_1 * (X_{r,:} - X_{i,:}) + r_2 * (gbest_j - X_{i,j}) \quad (7)$$

where i = 1 to N; j = 1 to D, $r = r_1 = r_2$= random number ~ U (0,1)

In this paper, the initial algorithm parameters are assigned based on the paper [23]. Other parameters are assigned as follows; the group size=thirty, the D=three, the number of run is fixed as 1000 and terminating criterion=$f(T)$.

2.2. Post-processing

This phase is responsible to extort tumor region from thresholded brain picture. To enhance segmentation accuracy, post-processing stage consist two sub-operations like the morphology based enhancement and segmentation.

2.2.1. Morphology

Picture level morphology is usually approved to enhance the exterior of illustration. The essential morphological functions, such as stroke organizational constituent (*strel*) and image fill (*imfill*) are used to enhance edges and illustration of multi-thresholded pictures.

2.2.2. Active contour segmentation

This section highlights LAC discussed in [16] to extort tumour.

The energy function of the snake is:

$$\frac{min}{C} \left\{ E_{GAC}(C) = \int_0^{L(C)} g(\left| \nabla I_0 C(s) \right| ds \right\} \quad (8)$$

where ds=Euclidean component of length and $L(C)$=length of arc C which satisfies $L(C) = \int_0^{L(C)} ds$. The parameter g=edge pointer.

This procedure is mathematically represented as:

$$\partial_t C = (kg - \left\langle \nabla_g , N \right\rangle) N \quad (9)$$

where $\partial_t C = \partial C / \partial t$ =deformation in the snake model, t=iteration time, and k, N are curvature and normal for the snake 'C'. Other details are exists in [20-22].

2.2.3. Related segmentation approaches

Along with the active contour segmentation, the well-known approaches, such as the Watershed (WS) and Level Set (LS) methods are also considered in this paper to segment the tumor region. The WS is a commonly considered in image mining approaches due to its simplicity and superiority [24]. The WA consists: (i) Sobel border recognition, (ii) Marker inhibited morphological operation, and (iii) Segmentation. Detail of WA is in [25]. The main benefit of LS contrast to other approach is, it creates shapes of combined topology to hold tearing and joining action during the picture outline examination. The LS proposed by Li et al. [26] is employed to extract the tumor by using a single well approach. The LS is a semi-automated technique and requires a bounding box initialization with respect to the width and height of the stroke section [27, 28]

2.2.4. Investigation

Competence implemented system is confirmed in the pre-processing phase and segmentation phase. During first phase, well-known image quality measures are computed to find the performance of SGO + Tsallis [7, 8]. After the segmentation, a relative investigation between segmented tumor and GT is achieved and statistical picture trials are calculated to examine the dominance of the implemented scheme [17]. Maximized standards of these constraints are usually believed to validate the importance of the proposed scheme [29, 30].

The mathematical expressions for the image similarity and statistical measures are presented below. During this examination, similarity constraints, like Jaccard, Dice, FPR, and FNR as well as the statistical constraints, as Sensitivity, Specificity, Accuracy and Precision are computed [19-22].

These events can be indicated as follows:

$$\mathrm{JI} = I_G \cap I_{SE} / I_G \cup I_{PP} \tag{10}$$

$$DC = 2(I_G \cap I_{PP}) / |I_G| \cup |I_{PP}| \tag{11}$$

$$\text{Sensitivity} = T_P / (T_P + F_N) \tag{12}$$

$$\text{Specificity} = T_N / (T_N + F_P) \tag{13}$$

$$\text{Accuracy} = (T_P + T_N) / (T_P + T_N + F_P + F_N) \tag{14}$$

$$\text{Precision} = T_P / (T_P + F_P) \tag{15}$$

where I_G is ground truth image, I_{PP} is post-processed image [19-22].

3. Realization

Primarily, SGO values are fixed as follows; group size=30, *D*=3 and total iteration=1000. In experimental investigation, each MRI slice is separately examined with the implemented method.

Figure 1 depicts pictorial representation of MRI assessment job. Initially, the skull stripped brain MRI picture is pre-processed by multi-thresholding. Afterwards, the image morphological operation is considered to group the similar image pixels in order to get a smooth image. Post-processed picture is processed with ACS. Finally, analysed and result is validated.

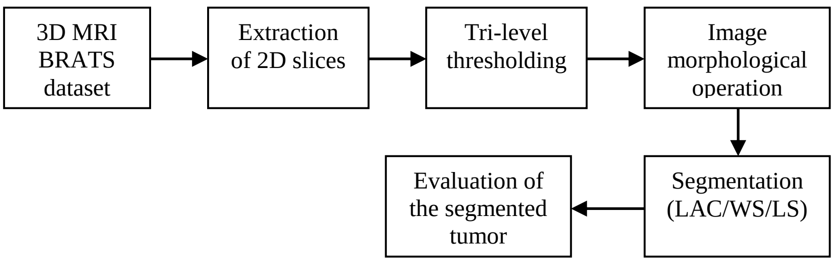

Fig. 1. Diagram of the proposed computerised tool.

4. Results and Discussions

Proposed procedure is tested using MICCAI BRAIN Tumor Segmentation (BRATS) challenge database [31]. It supports modalities, such as T2, T1 and T1c. This dataset also provides GT images for each slice. Initially, brain MRI recorded with Flair modality is considered and 2D slices with numbers 95,105,115 and 125 are extracted from the 3D dataset. Initially, SGO+TE multi-thresholding is executed on chosen slices. After the thresholding, image morphology is applied to group the similar pixels values to obtain an even image. The ACS process is then used to mine tumor part from the post-processed picture. Finally, the extracted tumor core is verified with GT using a relative study.

Table 1 presents the chosen image slices and its corresponding outcomes. The quality of the pre-processed image is verified using picture excellence measures active in the literature [29, 30, 32] and its values are tabulated in Table 2. From this table, the values of RMSE, PSNR, SSIM, NCC, AD, SC and NAE are noted. Details regarding the adopted image quality measures can be found in the literatures [7, 8].

Table 1. Image processing results for the chosen image dataset.

	Test image	**Pre-processing**	**Post-processing**	**Segmentation**
Slice$_{95}$	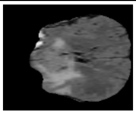	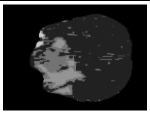	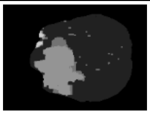	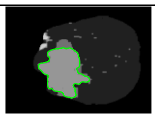
Slice$_{105}$	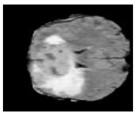	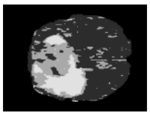	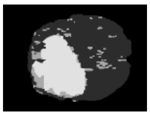	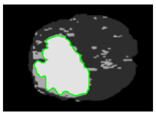
Slice$_{115}$		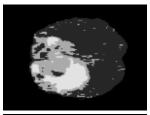	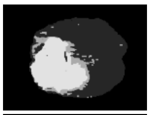	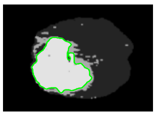
Slice$_{125}$	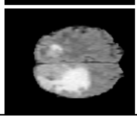	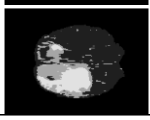	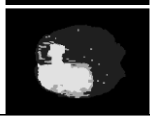	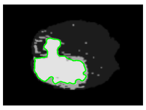

Table 2. Image quality measures between original and tri-level threshed image.

Flair	**RMSE**	**PSNR**	**SSIM**	**NCC**	**AD**	**SC**	**NAE**
Slice95	30.76	18.36	0.71	0.65	17.08	1.90	0.42
Slice105	43.99	15.26	0.68	0.73	22.79	1.56	0.36
Slice115	44.56	15.15	0.70	0.71	21.88	1.59	0.38
Slice125	43.10	15.44	0.72	0.69	19.54	1.62	0.41
Mean	40.60	16.05	0.70	0.69	20.32	1.67	0.39

Table 3 presents the extracted tumor section with LAC, WS and LS segmentation procedures. The comparison between the GT and extracted tumor results, such as picture resemblance measures and arithmetical measures are presented in Tables 4 and 5 respectively for LAC alone and approximately similar results are obtained with the WS and the LS techniques. From Table 4, one can observe that, the Jaccard and Dice values are greater than 0.82 (i.e., 82%) and also a negligible values for the FPR and FNR. This confirms that, the extracted tumor structure is roughly related to GT picture. The pattern of the tumor and the ground truth are identical. From Table 5, it can be noted that, all the measures are greater that 0.95 (i.e., 95%), which authenticates the superiority of proposed method in processing the benchmark Flair modality based brain MRI dataset.

Table 6 presents the average performance measures obtained with the considered segmentation procedures and the pictorial representation of this comparison is also presented in Fig. 2. This confirms that, results offered by the LAC segmentation are comparatively better than the WS and LS methods. To validate the superiority of implemented technique, other test images existing in the BRATS 2015 can also be considered for the examination. From this dataset, the flair and T2 modality pictures are considered and satisfactory results are obtained with the proposed SGO+LAC approach. From this, it is confirmed that, projected computerised apparatus works well for flair and T2 modalities.

Table 3. Comparison of the ground truth and the extracted tumor.

Test image	Ground truth	Tumor section		
		LAC	WS	LS
Slice_{95}				
Slice_{105}				
Slice_{115}			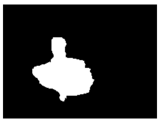	
Slice_{125}				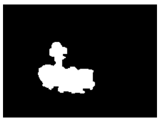

Table 4. Similarity measures between GT and segmented tumor (with LAC).

Flair	Jaccard	Dice	FPR	FNR
Slice_{95}	0.8340	0.9095	0.1526	0.0387
Slice_{105}	0.8291	0.9066	0.1674	0.0321
Slice_{115}	0.8397	0.9129	0.1368	0.0454
Slice_{125}	0.8221	0.9024	0.1147	0.0836
Mean	0.8311	0.9078	0.1429	0.0499

Table 5. Statistical measures between GT and segmented tumor (with LAC).

Flair	Precision	Sensitivity	Specificity	Accuracy
Slice$_{95}$	0.9963	0.9857	0.9612	0.9734
Slice$_{105}$	0.9955	0.9768	0.9679	0.9723
Slice$_{115}$	0.9937	0.9812	0.9546	0.9678
Slice$_{125}$	0.9910	0.9877	0.9554	0.9514
Mean	0.9941	0.9828	0.9598	0.9662

Table 6. Mean values of performance measures attained with LAC, WS and LS.

Approach	Jaccard	DIce	Precision	Sensitivity	Specificity	Accuracy
LAC	0.8311	0.9078	0.9941	0.9828	0.9598	0.9662
WS	0.8305	0.9032	0.9937	0.9815	0.9562	0.9659
LS	0.8309	0.9051	0.9928	0.9822	0.9571	0.9660

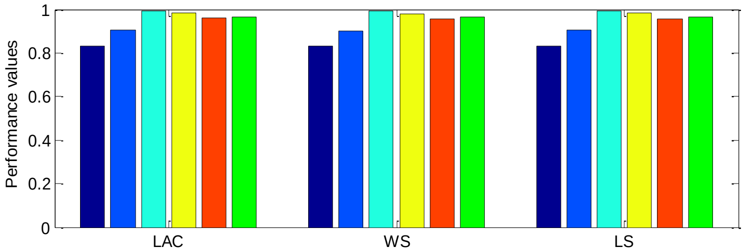

Fig. 2. Comparison of obtained picture likeliness values.

5. Conclusions

This work proposes a processor assisted system to mine and examine abnormal region of the BRATS 2012 brain MRI dataset. The work implements the SGO and TE based procedure to enhance the tumor section and the Active Contour method to segment the tumor from the post-processed test image. To display the advantage of proposed tool, Flair modality 2D slices are considered. The investigational outcome reveals that, projected technique is very efficient in extracting the tumor of Flair MRI. This result also confirms that, SGO assisted method offers better image similarity and statistical values compared to the GT with better accuracy.

Abbreviations

FNR	False negative rate
FPR	False positive rate
LAC	Localised active contour
LS	Level set segmentation
MRI	Magnetic resonance images
SGO	Social group optimization
WS	Watershed algorithm

References

1. Abdel-Maksoud, E.; Elmogy, M.; and Al-Awadi, R. (2015). Brain tumor segmentation based on a hybrid clustering technique. *Egyptian Informatics Journal*, 16(1), 71-81.
2. Abdullah, A.A.; Chize, B.S.; and Zakaria, Z. (2012). Design of cellular neural network (CNN) simulator based on Matlab for brain tumor detection. *Journal of Medical Imaging and Health Informatics*, 2(3), 296-306.
3. Bauer, S.; Wiest, R.; Nolte, L.-P.; and Reyes, M. (2013). A survey of MRI-based medical image analysis for brain tumor studies. *Physics in Medicine & Biology*, 58(13), R97.
4. Sezgin, M.; and Sankar, B. (2004). Survey over image thresholding techniques and quantitative performance evaluation. *Journal of Electronic Imaging*, 13(1), 146-165.
5. Lakshmi, V.S.; Tebby, S.G.; Shriranjani, D.; and Rajinikanth, V. (2016). Chaotic cuckoo search and Kapur/Tsallis approach in segmentation of T. Cruzi from blood smear images. *International Journal of Computer Science and Information Security (IJCSIS)*, 14(CIC2016_Paper 108), 51-56.
6. Rajinikanth V.; and Couceiro, M.S. (2015). RGB histogram based color image segmentation using firefly algorithm. *Procedia Computer Science*, 46, 1449-1457.
7. Rajinikanth, V.; Dey, N.; Satapathy, S.C.; and Ashour, A.S. (2018). An approach to examine magnetic resonance angiography based on Tsallis entropy and deformable snake model. *Future Generation Computer Systems*, 85, 160-172.
8. Raja, N.S.M.; Rajinikanth, V.; and Latha, K. (2014). Otsu based optimal multilevel image thresholding using firefly algorithm. *Modelling and Simulation in Engineering*, Vol. 2014, Article ID 794574, 17 pages.
9. Tsallis, C. (1988). Possible generalization of Boltzmann-Gibbs statistics. *Journal of Statistical Physics*, 52(1-2), 479-487.
10. Tsallis, C. (2002). Entropic nonextensivity: a possible measure of complexity. *Chaos, Solitons & Fractals*, 13(3), 371-391.
11. Akay, B. (2013). A study on particle swarm optimization and artificial bee colony algorithms for multilevel thresholding. *Applied Soft Computing*, 13(6), 3066-3091.
12. Manic, K.S.; Priya, R.K.; and Rajinikanth, V. (2016). Image multithresholding based on Kapur/Tsallis entropy and firefly algorithm. *Indian Journal of Science and Technology*, 9(12), 1-6.
13. Rajinikanth, V.; Raja, N.S.M.; and Kamalanand, K. (2017). Firefly algorithm assisted segmentation of tumor from brain MRI using Tsallis function and Markov random field. *Journal of Control Engineering and Applied Informatics*, 19(3), 97-106.
14. Despotović, I.; Goossens, B.; and Philips, W. (2015). MRI segmentation of the human brain: challenges, methods, and applications. *Computational and Mathematical Methods in Medicine*, Vol. 2015, Article ID 450341, 23 pages.
15. Tuba, M. (2014). Multilevel image thresholding by nature-inspired algorithms: A short review. *Computer Science Journal of Moldova*, 22(3), 318-338.

16. Bresson, X.; Esedoglu, S.; Vandergheynst, P.; Thiran, J.P. and Osher, S. (2007). Fast global minimization of the active contour/snake model. *Journal of Mathematical Imaging and Vision*, 28(2), 151-167.
17. Chaddad, A.; and Tanougast, C. (2016). Quantitative evaluation of robust skull stripping and tumor detection applied to axial MR images. *Brain Informatics*, 3(1), 53-61.
18. Lu, H.; Kot, A.C.; and Shi, Y.Q. (2004). Distance-reciprocal distortion measure for binary document images. *IEEE Signal Processing Letters*, 11(2), 228-231.
19. Varsha Shree, T.D.; Revanth, K.; Raja, N.S.M.; and Rajinikanth, V. (2018). A hybrid image processing approach to examine abnormality in retinal optic disc. *Procedia Computer Science*, 125, 157-164.
20. Rajinikanth, V.; and Satapathy, S.C. (2018). Segmentation of ischemic stroke lesion in brain MRI based on social group optimization and fuzzy-Tsallis entropy. *Arabian Journal for Science and Engineering*, 43(8), 4365-4378.
21. Rajinikanth, V.; Satapathy, S.C.; Fernandes, S.L.; and Nachiappan, S. (2017). Entropy based segmentation of tumor from brain MR images - A study with teaching learning based optimization. *Pattern Recognition Letters*, 94, 87-95.
22. Dey, N.; Rajinikanth, V.; Ashour, A.S.; and Tavares, J.M.R.S. (2018). Social group optimization supported segmentation and evaluation of skin melanoma images. *Symmetry*, 10(2), 51.
23. Satapathy, S.; and Naik, A. (2016). Social group optimization (SGO), A new population evolutionary optimization technique. *Complex & Intelligent Systems*, 2(3), 173-203.
24. Kaleem, M.; Sanaullah, M.; Hussain, M.A.; Jaffar, M.A.; and Choi, T.S. (2012). Segmentation of brain tumor tissue using marker controlled watershed transform method. *Communications in Computer and Information Science*, 281, 222-227.
25. Deng, G.; and Li, Z. (2012). An improved marker-controlled watershed crown segmentation algorithm based on high spatial resolution remote sensing imagery. *Recent Advances in Computer Science and Information Engineering*, *Lecture Notes in Electrical Engineering*, 128, 567-572.
26. Li, C.; Xu, C.; Gui, C.; and Fox, M.D. (2010). Distance regularized level set evolution and its application to image segmentation. *IEEE Transactions on Image Processing*, 19(12), 3243-3254.
27. Rajinikanth, V. Raja, N.S.M. Satapathy, S.C.; and Fernandes, S.L. (2017). Otsu's multi-thresholding and active contour snake model to segment dermoscopy images. *Journal of Medical Imaging and Health Informatics*, 7(8), 1837-1840.
28. Raja, N.S.M.; Rajinikanth, V.; Fernandes, S.L.; and Satapathy, S.C. (2017). Segmentation of breast thermal images using Kapur's entropy and hidden Markov random field. *Journal of Medical Imaging and Health Informatics*, 7(8), 1825-1829.
29. Satapathy, S.C.; Raja, N.S.M.; Rajinikanth, V.; Ashour, A.S.; and Dey, N. (2016). Multi-level image thresholding using Otsu and chaotic bat algorithm. *Neural Computing and Applications*, 29(12), 1285-1307.

30. Rajinikanth, V.; and Couceiro, M.S. (2015). Optimal multilevel image threshold selection using a novel objective function. *Advances in Intelligent Systems and Computing*, 340, 177-186.
31. Brain Tumor Database (BraTS-MICCAI). Retrieved October 5, 2017, from http://hal.inria.fr/hal-00935640.
32. Rajinikanth, V.; Raja, N.S.M.; and Satapathy, S.C. (2016). Robust color image multi-thresholding using between-class variance and cuckoo search algorithm. *Advances in Intelligent Systems and Computing*, 433, 379-386.